Mesothelial cells give rise to hepatic stellate cells and myofibroblasts via mesothelial–mesenchymal transition in liver injury

Yuchang Li, Jiaohong Wang, and Kinji Asahina[1]

Southern California Research Center for Alcoholic Liver and Pancreatic Diseases and Cirrhosis and Department of Pathology, Keck School of Medicine of the University of Southern California, Los Angeles, CA 90089

Edited by Brigid L. M. Hogan, Duke University Medical Center, Durham, NC, and approved December 28, 2012 (received for review August 22, 2012)

In many organs, myofibroblasts play a major role in the scarring process in response to injury. In liver fibrogenesis, hepatic stellate cells (HSCs) are thought to transdifferentiate into myofibroblasts, but the origins of both HSCs and myofibroblasts remain elusive. In the developing liver, lung, and intestine, mesothelial cells (MCs) differentiate into specific mesenchymal cell types; however, the contribution of this differentiation to organ injury is unknown. In the present study, using mouse models, conditional cell lineage analysis has demonstrated that MCs expressing Wilms tumor 1 give rise to HSCs and myofibroblasts during liver fibrogenesis. Primary MCs, isolated from adult mouse liver using antibodies against glycoprotein M6a, undergo myofibroblastic transdifferentiation. Antagonism of TGF-β signaling suppresses transition of MCs to mesenchymal cells both in vitro and in vivo. These results indicate that MCs undergo mesothelial–mesenchymal transition and participate in liver injury via differentiation to HSCs and myofibroblasts.

Epithelial-mesenchymal transition | fibrosis | Glisson's capsule | podoplanin | alpha-smooth muscle actin

Mesothelial cells (MCs) form a single squamous epithelial cell layer and cover the surfaces of the internal organs, as well as the walls of cavities (1, 2). MCs have a phenotype intermediate between epithelial and mesenchymal cells, expressing markers indicative of both cell types. Recent studies in patients with peritoneal fibrosis following peritoneal dialysis for treatment of kidney failure suggest that peritoneal MCs undergo epithelial mesenchymal transition (EMT) and give rise to myofibroblasts (3). EMT is a process by which epithelial cells lose their polarity and gain migratory capacity in embryogenesis, tissue repair, organ fibrosis, and tumor invasion and metastasis (4). TGF-β signaling, implicated in EMT, suppresses expression of E-cadherin (CDH1), Zo1 (TJP1), and cytokeratin (KRT) while inducing vimentin (VIM) and α-smooth muscle actin (ACTA2) in peritoneal MCs (3, 5).

MCs covering the Glisson's capsule of the liver have microvilli protruding into the peritoneal cavity (6). Little is known, however, about the function and differentiation potential of liver MCs during wound healing. Our previous cell lineage analysis revealed that MesP1^{+} mesoderm gives rise to the majority of liver MCs as well as parietal MCs of the peritoneal cavity (7). In mouse embryonic livers, MCs express podoplanin (PDPN), activated leukocyte cell adhesion molecule (ALCAM), and Wilms tumor 1 (WT1) (7). Conditional cell lineage tracing using Wt1^{CreERT2}; Rosa26^{flox} (R26^{f}) reporter mice demonstrated that the Wt1^{+} mesothelium migrates inward from the liver surface and gives rise to hepatic stellate cells (HSCs), fibroblasts, and smooth muscle cells during liver morphogenesis (8). In addition, embryonic MCs may support proliferation of hepatoblasts by secretion of hepatocyte growth factor (HGF) and pleiotrophin (PTN) (9, 10). These results indicate that MCs are progenitor cells of liver mesenchymal cells and play a role in hepatogenesis. Similar to what has been observed during liver development, MCs have been shown to act as mesenchymal progenitor cells in the developing lung, intestine, and heart (11–13). It remains to be clarified, however, whether or not MCs have a similar differentiation potential in tissue injury and regeneration in the adult.

Liver fibrosis is a scarring process characterized by deposition of excessive fibrous tissues (14). Alcohol abuse and chronic hepatitis C virus (HCV) infection often cause fibrosis and cirrhosis. In the adult liver, HSCs are recognized as the main fibrogenic cell type (15). HSCs are characterized by the expression of desmin (DES), glial fibrillary acidic protein (GFAP), and VIM, as well as by accumulation of vitamin A-storing lipid droplets and having dendritic processes along the sinusoid. Upon liver injury, HSCs transform into a myofibroblastic phenotype expressing ACTA2 and synthesize excessive extracellular matrix proteins. Although activation of HSCs is believed to be key in the development of myofibroblasts, several lines of evidence suggest there are actually several sources of myofibroblasts in liver fibrogenesis (16, 17). Electron microscopic studies suggest that myofibroblasts are also derived from fibroblasts around the central vein or in the Glisson's capsule (18). The origins and relative contributions of these mesenchymal cell types in liver fibrogenesis are, however, unknown.

In the present study, we examined the differentiation potential of MCs in the adult liver. Based on the expression of glycoprotein M6a (GPM6A), we isolated MCs from adult liver and found that liver MCs lose the MC phenotype and acquire a mesenchymal cell phenotype through TGF-β signaling. Using conditional cell lineage tracing in Wt1^{CreERT2} mice, we demonstrated that MCs can generate both HSCs and myofibroblasts depending on injury signals in the liver. We propose that, during liver fibrogenesis, MCs differentiate into mesenchymal fibrogenic cells via what we now refer to as mesothelial–mesenchymal transition (MMT).

Results

Specific Expression of GPM6A in Liver MCs. Our previous studies in mouse embryos demonstrated that MCs covering the liver surface migrate inward and give rise to HSCs, fibroblasts, and vascular smooth muscle cells (8). This finding raised questions about whether MCs in the adult liver have a similar differentiation potential during injury or regeneration. We previously identified PDPN as an MC marker in embryonic liver (7). In the adult liver, however, PDPN was expressed not only in MCs, but also in bile duct and lymphatic vessels (Fig. 1 *C* and *D*). To identify specific MC markers in the adult mouse liver, we purified MCs from E12.5 embryonic livers by FACS using anti-PDPN antibodies

Author contributions: K.A. designed research; Y.L., J.W., and K.A. performed research; Y.L. and K.A. analyzed data; and K.A. wrote the paper.

The authors declare no conflict of interest.

This article is a PNAS Direct Submission.

Data deposition: The data reported in this paper have been deposited in the Gene Expression Omnibus (GEO) database, www.ncbi.nlm.nih.gov/geo (accession no. GSE39064).

[1]To whom correspondence should be addressed. E-mail: asahina@usc.edu.

This article contains supporting information online at www.pnas.org/lookup/suppl/doi:10.1073/pnas.1214136110/-/DCSupplemental.

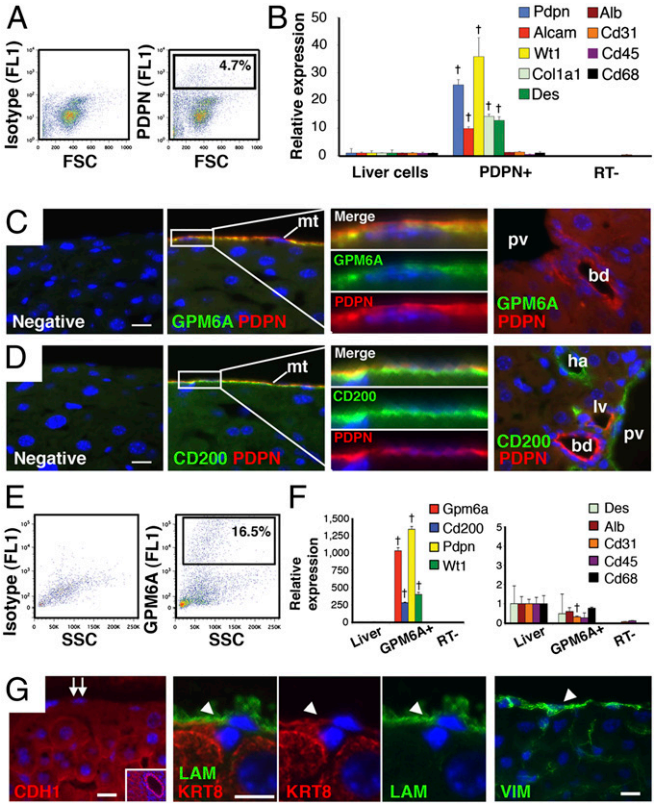

Fig. 1. Identification of GPM6A as a liver MC-specific marker. (*A*) PDPN$^+$ cells (4.7%) were sorted from E12.5 mouse embryonic livers using FACS and anti-PDPN antibodies. Isotype IgG was used as a negative control. (*B*) QPCR of the purified E12.5 PDPN$^+$ cells and liver cells. $^\dagger P < 0.01$ compared with liver cells. (*C* and *D*) Immunostaining of PDPN (red) and GPM6A or CD200 (green) in normal adult mouse livers. The surface mesothelium (mt) expresses PDPN, GPM6A, and CD200. The last panels show the portal area inside the liver. Immunostaining without the first antibody was used as negative controls. bd, bile duct; ha, hepatic artery; lv, lymphatic vessel; pv, portal vein. (*E*) GPM6A$^+$ cells (16.5%) were sorted from adult mouse liver cells using FACS and anti-GPM6A antibodies. (*F*) QPCR of purified GPM6A$^+$ cells in adult livers. $^\dagger P < 0.01$ compared with liver cells. (*G*) Immunostaining of CDH1, LAM, KRT8, and VIM in adult mouse liver. MCs are negative for CDH1 (double arrows). Positive staining of CDH1 in the bile duct (*Inset*). Arrowheads indicate MCs expressing LAM, KRT8, and VIM. Nuclei were counterstained with DAPI. (Scale bar, 10 μm.)

(Fig.1*A*) and then surveyed gene expression by microarray analysis. The E12.5 PDPN$^+$ population was shown to express MC markers, such as *Pdpn*, *Alcam*, and *Wt1* (Fig. 1*B*), validating successful purification of MCs. These PDPN$^+$ MCs also expressed *Col1a1* and *Des*, but not markers for hepatoblasts (*Alb*), endothelial cells (*Cd31*), or blood cells (*Cd45* and *Cd68*) (Fig. 1*B*). Microarray analysis comparing E12.5 PDPN$^+$ MCs and liver cells revealed high expression of *Pdpn*, *Wt1*, *Alcam*, *Podxl*, *Cd200*, and *Gpm6a* in MCs (Fig. S1*A*). CD200 is a ligand for CD200 receptors (19). GPM6A is a member of the proteolipid protein family and was previously reported to be a marker for the epicardium that is the MC layer in developing heart (20, 21). Quantitative PCR (QPCR) confirmed the high expression of *Cd200* and *Gpm6a* in E12.5 PDPN$^+$ MCs (Fig. S1*B*). Immunostaining also showed specific expression of GPM6A and CD200 in PDPN$^+$ MCs in the E12.5 fetal livers (Fig. S1*C*).

We also examined expression of GPM6A and CD200 by immunostaining in the adult liver. GPM6A was only expressed in MCs on the liver surface, whereas CD200 was expressed in MCs and endothelial cells in the portal vein and hepatic artery (Fig. 1 *C* and *D*). Having identified GPM6A as a specific MC marker, we isolated MCs from the adult liver by FACS using anti-GPM6A antibodies. After digestion of the liver surface, 16.5% of the cells were positive for GPM6A (Fig. 1*E*). QPCR showed the GPM6A$^+$ population expressed MC-specific markers (*Gpm6a*, *Cd200*, *Pdpn*, and *Wt1*), but other cell markers were expressed to a lesser extent (*Alb*, *Cd31*, *Cd45*, and *Cd68*), indicating successful isolation of MCs (Fig. 1*F*). We also characterized known MC markers in the liver by immunostaining. CDH1 is widely used as a marker for epithelial cells and MCs (1–3); however, in adult liver, CDH1 was expressed in hepatocytes and biliary epithelial cells, but not in MCs (Fig. 1*G*). Liver MCs expressed laminin (LAM), KRT8, and VIM (Fig. 1*G*), implying that MCs have an intermediate phenotype between epithelial cells and mesenchymal cells in normal mouse liver.

Mesothelial–Mesenchymal Transition in Culture. To characterize liver MCs, we isolated MCs from the adult liver using anti-GPM6A antibodies and magnetic beads. This method allowed us to isolate 1.2–1.4 × 10^5 MCs from five mice. The isolated MCs were plated at a density of 2 × 10^4 cells per well of a 24-well plate and they slowly attached over 2–3 d. The plated MCs formed epithelial cell colonies and became confluent within 1 wk (Fig. 2*A*). From 1 wk after plating, some MCs lost epithelial cell polarity and became fibroblastic cells (Fig. 2*A*). Following two passages, neither epithelial nor fibroblastic MCs attached to the dish and survived.

Cultured MCs showed decreased mRNA expression of both MC markers (*Gpm6a*, *Pdpn*, *Cd200*, and *Wt1*) and epithelial cell markers (*Gja1*, *Tjp1*, and *Krt8*) (Fig. 2*B*). Consistent with the lack of CDH1 expression in liver MCs (Fig. 1*G*), the mRNA expression level of *Cdh1* was almost undetectable in cultured MCs (Fig. 2*B*). Cultured MCs increased expression of *Acta2*, *Col1a1*, and *Des* (Fig. 2*B*), suggesting a change in phenotype from epithelial to mesenchymal. MCs expressed *Vim* in the normal liver (Fig. 1*G*), but this mRNA expression was decreased in culture (Fig. 2*B*). EMT driver genes including *Snail* and *Twist* were weakly expressed in MCs, but that expression was not up-regulated throughout the culture period (Fig. 2*B*). Isolated MCs continued expressing *Tgfb1* and *Tgfb3* (Fig. S2*A*). Cultured MCs increased expression of *Egfr* (Fig. S2*A*). MCs down-regulated expression of *Ptn* in culture and they did not express *Hgf* (Fig. S2*A*). Cultured MCs did not increase expression of *Alb*, *Cd31*, *Cd68*, and *Cd45* (Fig. S2*A*). These data indicate spontaneous differentiation of liver MCs to mesenchymal cells in vitro. Because MCs express both epithelial and mesenchymal cell markers in the normal liver, we describe the transition of MCs to mesenchymal cells as MMT rather than EMT.

TGF-β Induces MMT of Liver MCs. To test whether known EMT inducers, such as EGF, HGF, AngII, TGF-β, retinoic acid (RA), WNT3A, and DKK1 (a WNT inhibitor) (4, 22), promote a conversion of liver MCs to mesenchymal cells, we treated primary cultured MCs with each one of these factors for 4 d (from days 1 to 5). TGF-β most notably suppressed the MC marker (*Gpm6a*) while inducing mesenchymal cell markers (*Acta2*, *Col1a1*, and *Vim*) (Fig. 3*A*). TGF-β also suppressed expression of epithelial cell markers (*Gja1* and Tjp1), but not *Krt8* (Fig. 3*A*).

To dissect the TGF-β signaling pathway in MCs, we treated MCs with TGF-β in the presence of various inhibitors for 4 d. SB431542, a specific inhibitor for TGF-βR1, reversed the down-regulation of *Gpm6a* and the up-regulation of *Acta2* and *Col1a1* caused by TGF-β (Fig. S2*B*). A chemical inhibitor for SMAD3 (SIS3) also suppressed the increased expression of *Acta2* and *Col1a1* without effect on expression of *Gpm6a* (Fig. S2*B*). p38, JNK, and ERK MAP kinases are known to be involved in a noncanonical TGF-β pathway (23). A p38 inhibitor (SB203580) weakly down-regulated the expression of *Acta2* induced by TGF-β (Fig. S2*B*). A MEK inhibitor (U0126) partially blocked the effect of TGF-β on *Acta2*. Inhibitors for JNK, mTOR, or PI3K reduced the proliferation of

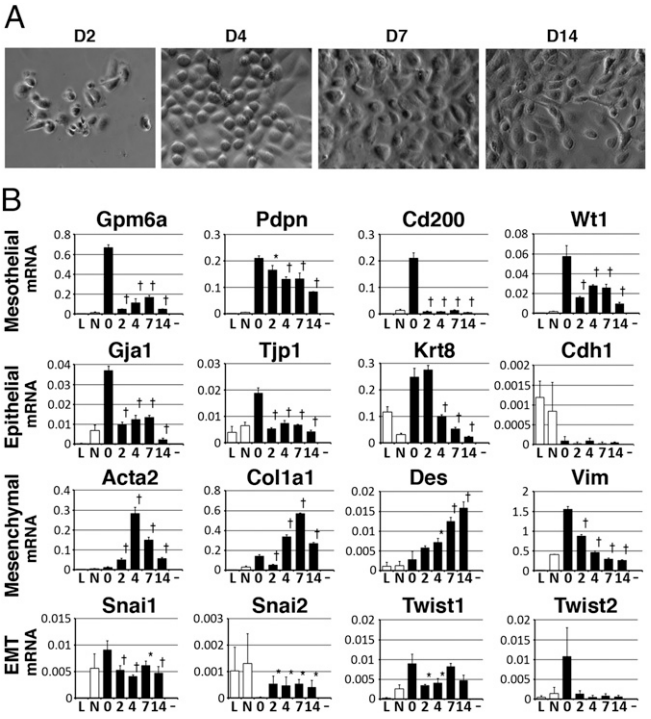

Fig. 2. Primary culture of liver MCs. MCs were purified from normal adult livers using anti-GPM6A antibodies and magnetic beads. (*A*) Morphology of primary liver MCs. (*B*) QPCR of MC, epithelial cell, mesenchymal cell, and EMT markers. Primary MCs decrease expression of MC and epithelial cell markers while increasing mesenchymal cell markers in culture. L, liver cells; N, GPM6A$^-$ population. $^*P < 0.05$, $^\dagger P < 0.01$ compared with isolated MCs (day 0).

MCs and increased expression of *Acta2* in the presence of TGF-β. These data suggest a canonical TGF-β pathway is involved in conversion of MCs to mesenchymal cells.

To analyze the TGF-β/SMAD3 pathway, we treated MCs with TGF-β in the presence or absence of chemical inhibitors from days 2–9. Long-term treatment with TGF-β suppressed expression of MC and epithelial cell markers (*Gpm6a*, *Gja1*, *Tjp1*, and *Krt8*) while inducing mesenchymal cell markers (*Acta2*, *Col1a1*, and *Vim*) (Fig. 3*B*). MCs changed from an epithelial morphology to a mesenchymal one in the presence of TGF-β (Fig. 3*C*). SB431542 blocked the increased expression of mesenchymal cell markers and decreased expression of MC and epithelial cell markers in the presence or absence of TGF-β (Fig. 3 *B*–*D*), suggesting autocrine TGF-β signaling also induces MCs to acquire a mesenchymal phenotype. Although to a lesser extent, SIS3 reversed conversion of MCs to mesenchymal cells in the presence of TGF-β (Fig. 3*B*). SIS3 treatment actually changed the morphology of MCs to flat epithelial cells (Fig. 3 *C* and *D*).

Cell Lineage Analysis of Wt1$^+$ Liver MCs. During primary MC culture, it is possible that contaminating fibroblastic cells might grow and differentiate into ACTA2$^+$ mesenchymal cells independent of the MMT of MCs. To rule out this possibility, we traced MC lineages using a Cre-loxP system. We found that some MCs specifically expressed WT1 in the adult liver surface (Fig. S3*A*). Wt1^{GFPCre} knock-in mice also showed specific expression of GFP in MCs (Fig. S3*B*). To conditionally trace WT1$^+$ MCs, we used Wt1^{CreERT2} knock-in and R26mTmG^{flox} (R26T/G^f) mice (Fig. 4*A*). The Wt1^{CreERT2} knock-in mouse expresses a fusion protein of Cre and ERT2 at the *Wt1* gene locus (13). Upon tamoxifen (TAM) treatment, the CreERT2 excises the Tomato sequence from the R26T/G^f locus and irreversibly induces membrane-tagged GFP expression (24). After TAM injection to adult Wt1^{CreERT2};R26T/G^f mice, 14.5% of MCs converted expression of Tomato to GFP at the liver surface (Fig. 4*B*). However, Wt1^{CreERT2};R26T/G^f mice without TAM injection or Wt1$^+$;R26T/G^f mice with TAM injection did not activate GFP expression (Fig. S3*C*), validating a tight control of the GFP expression by TAM.

Subsequent to labeling MCs as GFP$^+$ cells in Wt1^{CreERT2};R26T/G^f mice by TAM, we isolated these MCs and traced their phenotypes in culture. After plating, 38.3% of the cultured MCs expressed GFP in the epithelial colonies (Fig. S4*A*). The disparity in percentages of GFP$^+$ MCs in tissues (14.5%) versus in culture (38.3%) may be due to variable adherence of MCs to the dish or partial digestion of the liver surface for MC isolation. In culture, both GFP$^+$ and GFP$^-$ MCs expressed PDPN (Fig. S4*B*). Some of the GFP$^+$ and GFP$^-$ MCs started to express ACTA2 and TGF-β treatment induced ACTA2 expression in all GFP$^+$ or GFP$^-$ cells (Fig. S4*C*), demonstrating differentiation of MCs to mesenchymal cells in vitro. To rule out the possibility that TAM activates GFP expression in HSCs, we isolated HSCs from TAM-treated Wt1^{CreERT2};R26T/G^f mice and confirmed that there was no GFP expression in the vitamin A-storing HSCs (Fig. S4*D*).

MCs Give Rise to HSCs and Myofibroblasts in CCl_4-Induced Fibrosis. Next, we traced the lineages of Wt1$^+$ MCs in fibrotic liver. After labeling MCs as GFP$^+$ cells by TAM, liver fibrosis was induced by injection of CCl_4 1–30 times (Fig. 4*C*). One day after a single injection of CCl_4, GFP$^+$ MCs started to migrate inward from the liver surface and expressed DES, but not ACTA2 (Fig. 4*D*, double arrows). Three days after the single injection, 22.7% of GFP$^+$ cells inside the liver began to express ACTA2 and the percentage increased to 89.5% after three CCl_4 injections (Fig. 4*D*, arrows), indicating that liver injury caused by CCl_4 further induces transdifferentiation of MC-derived HSCs to myofibroblasts. After 30 injections, fibrotic septa composed of ACTA2$^+$ myofibroblasts were seen between the mesothelium and central vein (Fig. 4*E*). ACTA2$^+$ GFP$^+$ myofibroblasts were seen up to 150 μm in depth from the liver surface and there were no GFP$^+$ cells beyond this distance. Although 2.0% of ACTA2$^+$ myofibroblasts coexpressed GFP in the whole-liver sections, the percentage increased to 11.5% in the surface area within 150 μm in depth, indicating the contribution of MCs to myofibroblasts is restricted to near the liver surface. Given that the labeling efficiency of MCs by TAM was 14.5%, around 79% of ACTA2$^+$ myofibroblasts are likely derived from MCs within 150 μm in depth from the liver surface. The GFP$^+$ cells in the fibrotic septum coexpressed DES and type I collagen (Fig. S5*A*). There were no GFP$^+$ hepatocytes, cholangiocytes, or endothelial cells before or after CCl_4 treatment. Injections of mineral oil rather than CCl_4 did not induce MMT of MCs (Fig. S5*B*). We also confirmed that CCl_4 treatment did not induce GFP expression in Wt1^{CreERT2};R26T/G^f mice without TAM injection or in TAM-treated Wt1$^+$;R26T/G^f mice (Fig. S5*B*). Collectively, these data indicate that during CCl_4-induced fibrogenesis, MCs migrate inward from the liver surface, give rise to HSCs and then myofibroblasts, and form fibrotic septa connecting the mesothelium and central vein area.

To validate our results in R26T/G^f mice, we also used R26lacZ^f reporter mice (25) to trace MCs during fibrogenesis. After TAM injection of the Wt1^{CreERT2};R26lacZ^f mice, we specifically labeled MCs as LACZ$^+$ at the liver surface (Fig. S6 *A* and *B*). Following CCl_4 injections, LACZ signals were detected not only in MCs, but also in ACTA2$^+$ or DES$^+$ myofibroblasts beneath the MCs (Fig. S6 *C*–*F*), validating our conclusion that MCs differentiate into ACTA2$^+$ myofibroblasts during liver fibrosis.

Antagonism of TGF-β Signaling Suppresses Migration and Differentiation of MCs. Given that TGF-β was shown to be responsible for MMT of MCs in culture, we tested whether inhibition of TGF-β signaling

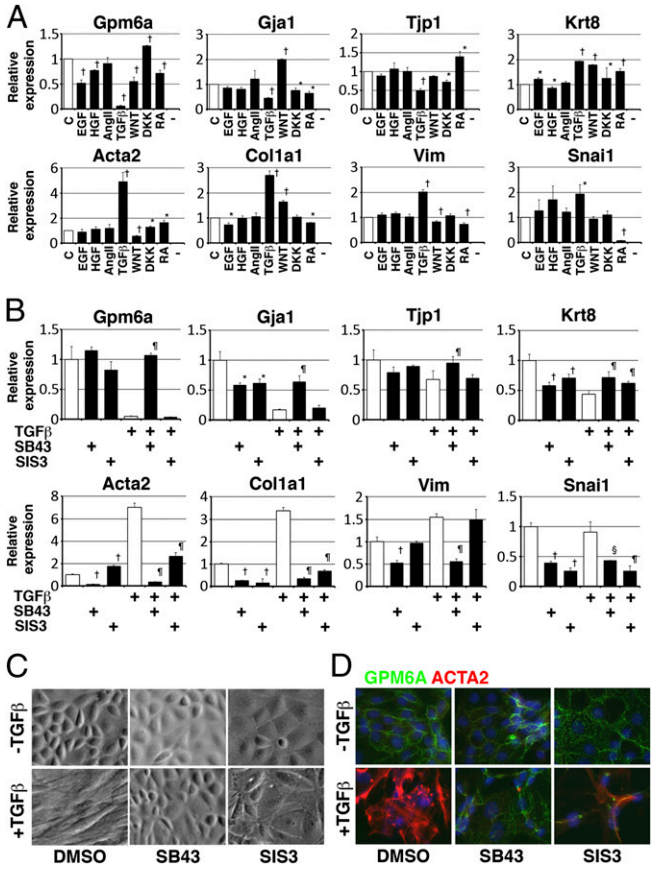

Fig. 3. Conversion of MCs to mesenchymal cells by TGF-β in vitro. Primary MCs were cultured in the presence or absence of cytokines and chemical inhibitors. (*A*) QPCR of MCs treated with indicated factors 4 d (from days 1–5). TGF-β induces expression of mesenchymal cell markers while suppressing *Gpm6a* and many epithelial cell markers (not *Krt8*). $^{*}P < 0.05$, $^{\dagger}P < 0.01$ compared with MCs without treatment (c, control). (*B*) QPCR of MCs treated with TGF-β and/or inhibitors for 7 d. TGF-β induces expression of mesenchymal cell markers while suppressing *Gpm6a*. TGF-β weakly suppresses expression of epithelial cell markers including *Krt8*. SB431542 (SB43: TGF-βR1 inhibitor) suppresses the effect of TGF-β on MCs. SIS3 (SMAD3 inhibitor) suppresses up-regulation of mesenchymal cell markers in MCs induced by TGF-β. $^{*}P < 0.05$, $^{\dagger}P < 0.01$ compared with no treatment. $^{\S}P < 0.05$, $^{\P}P < 0.01$ compared with TGF-β treatment. (*C* and *D*) Morphological and phenotypical changes in cultured MCs treated with TGF-β and/or inhibitors for 7 d. SB431542 keeps epithelial morphology and phenotype of MCs in the presence of TGF-β. SIS3 partially blocks morphological and phenotypical change of MCs by TGF-β.

suppresses MMT of MCs in the CCl_4 model. A soluble TGF-βR2 (STR) was previously shown to antagonize TGF-β1 and TGF-β3 and thereby inhibit liver fibrosis in mice (26). As outlined in Fig. 4*C*, we labeled MCs as GFP^+ by TAM, induced fibrosis by CCl_4 injections, and treated with STR or control IgG 12 times every 3 d. Compared with the control group, the STR treatment decreased the number of GFP^+ myofibroblasts inside the liver (Fig. 4*F*). The percentage of GFP^+ myofibroblasts in all GFP^+ cells including both MCs and myofibroblasts was significantly decreased from 41.4% (IgG) to 24.2% (STR) (Fig. 4*G*). These data indicate that, in fibrosis, TGF-β signaling is involved in migration and differentiation of MCs to myofibroblasts.

MCs Differentiate into HSCs in Biliary Fibrosis. Next, we tested the differentiation potential of MCs in biliary fibrosis induced by bile duct ligation (BDL) (Fig. 5*A*). One week after BDL, 4.5% of the GFP^+ MCs started migration from the liver surface (Fig. 5*B*, double arrows). GFP^+ cells were also located in the sinusoid and express DES near the liver surface (Fig. 5*B*, arrow). Three weeks after BDL, the GFP^+ DES^+ HSCs exhibited dendritic processes, a unique feature of HSCs (Fig. 5*C*). The GFP^+ HSCs expressed VIM and GFAP (Fig. 5*C*). In contrast to the CCl_4 model, the BDL model did not induce fibrosis beneath the mesothelium in 3 wk and MC-derived GFP^+ HSCs did not acquire the myofibroblastic phenotype; specifically, they did not express ACTA2 (Fig. 5*D*). The average distance from the liver mesothelium to the GFP^+ HSCs increased from 12.9 ± 8.6 μm (maximum 24 μm) at 1 wk to 33.1 ± 19.1 μm (maximum 132 μm) at 3 wk after BDL. We confirmed that BDL alone did not activate GFP expression in the mice without TAM treatment (Fig. S7*A*).

We also tested the effects of TGF-β signaling in MMT of MCs in biliary fibrosis. As outlined in Fig. S7*B*, we labeled MCs as GFP^+ cells, subjected the mouse to BDL, and treated with STR or control IgG every 3 d. Similar to observations in the CCl_4 model, the STR treatment inhibited migration of MCs (Fig. S7*C*) and the percentage of GFP^+ HSCs in all GFP^+ MCs and HSCs in the liver was significantly decreased from 33.9% (IgG) to 8.0% (STR) (Fig. S7*D*).

Negligible Contribution of MCs Differentiating to HSCs in Regenerating Livers. To test whether MCs in the adult liver have the potential to differentiate to HSCs during regeneration, we traced an MC lineage using a liver regeneration model induced by 70% partial hepatectomy (PHx) (Fig. S7*E*). Following PHx from 1 to 13 d, there was almost no GFP expression in the liver except in the MCs and GFP^+ DES^+ HSCs were only found at one to two cells per liver section (Fig. S7*F*), indicating a negligible contribution of MCs differentiating to HSCs during regeneration induced by PHx.

Discussion

MCs in the liver have been primarily considered as a protective barrier within the liver and their possible roles in liver injury and regeneration have never been addressed. Our previous study in mouse embryos revealed that MCs are progenitor cells capable of differentiating into HSCs, fibroblasts, and smooth muscle cells (8). The present study extended this observation to adult liver fibrosis and demonstrated that during the progression of liver fibrosis, liver MCs give rise to HSCs and myofibroblasts in response to injury signals. MCs in the normal liver expressed unique markers for MCs (*Gpm6a*, *Pdpn*, and *Cd200*) and traditional markers for epithelial cells (*Gja1*, *Tjp1*, and *Krt8*) as well as for mesenchymal cells (*Col1a1* and *Vim*), indicating that MCs have a mixed phenotype. Upon liver injury, MCs decreased expression of epithelial and MC markers and increased expression of mesenchymal cell markers. Because a majority of MCs are derived from mesoderm during liver development (7), MCs seem to be prone to acquire a mesenchymal phenotype by injury-associated stimuli. We described this conversion of liver MCs to mesenchymal cells as MMT instead of EMT.

Advanced liver fibrosis can lead to cirrhosis, portal hypertension, and liver cancer. Currently, there is no medical treatment for cirrhosis aside from liver transplantation (27). To develop a novel therapy for cirrhosis, it is essential to determine key cellular and molecular events responsible for the initiation and progression of liver fibrosis. During fibrogenesis, HSCs have been recognized as a major source of myofibroblasts; however, resident liver fibroblasts are also suggested to proliferate and form fibrotic septa (16–18). The present study has demonstrated that MCs undergo MMT and give rise to HSCs in both BDL and CCl_4 models. In the CCl_4 model, MCs first differentiated into HSCs and then acquired myofibroblastic phenotype expressing ACTA2. MC-derived myofibroblasts were seen in the fibrotic areas beneath the liver surface. It seems plausible that the injured hepatocytes near the central vein stimulate the region closest to the mesothelium and induce fibrosis. In our experimental condition, MC-

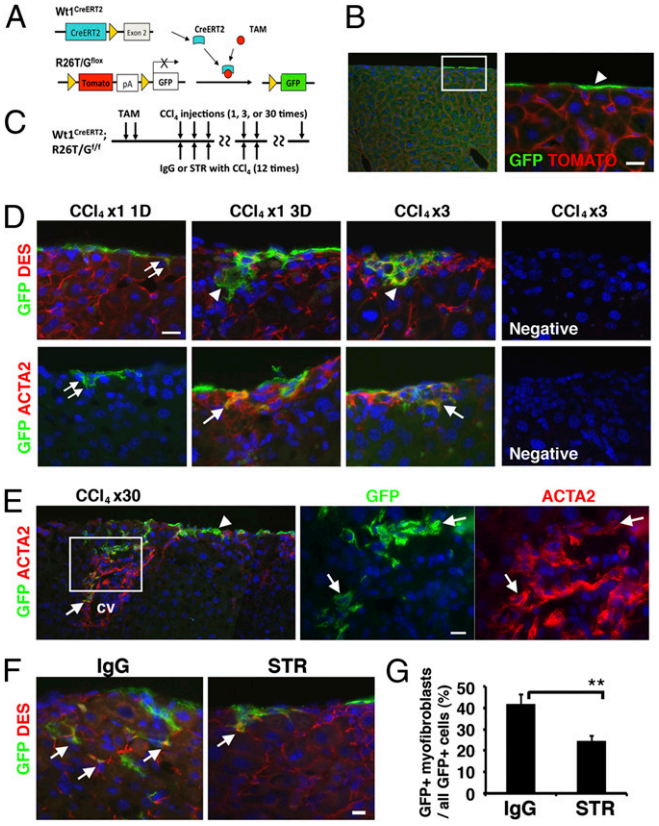

Fig. 4. Conditional MC lineage analysis in CCl_4-induced liver fibrosis. (*A*) After TAM injection, Wt1$^+$ MCs selectively convert expression of Tomato to membrane-tagged GFP in the Wt1^{CreERT2};R26T/G^f mouse liver. (*B*) Immunostaining of GFP in the liver 1 wk after TAM injections. Only MCs express GFP (arrowhead). (*C*) After labeling MCs by TAM injection, liver fibrosis was induced by CCl_4 injection 1–30 times. For inhibition of TGF-β signaling, mice were treated with CCl_4 injections 12 times and STR (TGF-βR2 Fc chimera) or IgG control for every 3 d. (*D*) Immunostaining of the liver for GFP, DES, and ACTA2. Double arrows indicate GFP$^+$ MCs differentiating into DES$^+$ ACTA2$^-$ HSCs 1 d after a single injection of CCl_4. Arrowheads and arrows indicate DES$^+$ GFP$^+$ and ACTA2$^+$ GFP$^+$ myofibroblasts, respectively. Immunostaining without the first antibody was used as negative controls. (*E*) Immunostaining of GFP and ACTA2 after injections of CCl_4 30 times. GFP$^+$ MCs (arrowhead) migrate inward from the liver surface and coexpress ACTA2 (arrows) in the fibrotic septum. cv, central vein. (*F*) Immunostaining for GFP and DES after injections of CCl_4 12 times cotreated with STR or control IgG. Arrows indicate DES$^+$ GFP$^+$ myofibroblasts derived from MCs. Nuclei were counterstained with DAPI. (Scale bar, 10 μm.) (*G*) Percentages of the GFP$^+$ myofibroblasts in all GFP$^+$ cells including both MCs and myofibroblasts in the control (IgG) and treated (STR) groups. Results are means ± SD of three mice. $^{**}P < 0.01$.

derived cells were seen near the liver surface. Although MCs contributed 2.0% of myofibroblasts in the CCl_4-induced liver fibrosis, the percentage increased to 11.5% near the surface area within 150 μm in depth, indicating that MC-derived myofibroblasts participate in "capsular fibrosis" of the liver surface. If we assume all MCs have the same differentiation potential and we consider that the labeling efficiency of MCs by TAM is 14.5%, around 79% of ACTA2$^+$ myofibroblasts are likely derived from MCs within 150 μm in depth from the liver surface in the CCl_4 model. MCs show heterogeneity in terms of Wt1 expression, however, and Wt1-negative MCs might not undergo MMT. Although further studies are necessary to address the pathological implications of capsular fibrosis compared with perivenular or perisinusoidal fibrosis, capsular fibrosis may involve an increase in the liver stiffness by deposition of collagen beneath the mesothelium. The liver mesothelium will be a potential therapeutic target for suppression of the capsular fibrosis by injecting drugs into the peritoneal cavity.

In contrast to observations made in the CCl_4 model, we found that BDL induced differentiation of MCs to HSCs, but not to ACTA2$^+$ myofibroblasts in 3 wk. We previously reported that BDL does not fully induce myofibroblastic conversion of HSCs (28). These observations may indicate that BDL does not provide sufficient stimulus to induce differentiation of MC-derived HSCs to myofibroblasts in mice.

Similar to observations made in vitro, antagonism of TGF-β signaling in both the CCl_4 and BDL models effectively suppressed differentiation of MCs to HSCs and myofibroblasts. During liver fibrogenesis, TGF-β plays a major role in activation of HSCs (26). Thus, the profibrogenic role of TGF-β is conserved in the process of activation of HSCs and MMT of MCs in injured livers. Liver regeneration induced by PHx did not induce differentiation of MCs to HSCs. Although it remains to be determined, our results imply that stimuli caused by liver injury, rather than regeneration, can trigger MMT of MCs and induce differentiation toward HSCs.

Activated HSCs are known to secrete HGF and PTN and support proliferation of hepatocytes (10). Our data suggest, however, that MCs do not express *Hgf* mRNA and reduce expression of *Ptn* throughout time in culture, implying that MC-derived myofibroblasts have less proregenerative influence on hepatocytes in injured liver.

In cancer invasion and metastasis, cancer cells are believed to acquire a migratory phenotype and lose the epithelial phenotype via EMT, which is triggered by many signals, including TGF-β (4). In liver MCs, an inhibitor of TGF-βR1 blocked MMT induced by TGF-β. In addition, a chemical inhibitor for SMAD3 also blocked MMT; however, inhibitors for p38, JNK, or ERK did not block MMT of MCs. Therefore, a canonical TGF-β/SMAD3 signaling is the principal mechanism for induction of liver MMT. Liver MCs expressed mRNAs for *Twist* and *Snail* at low levels,

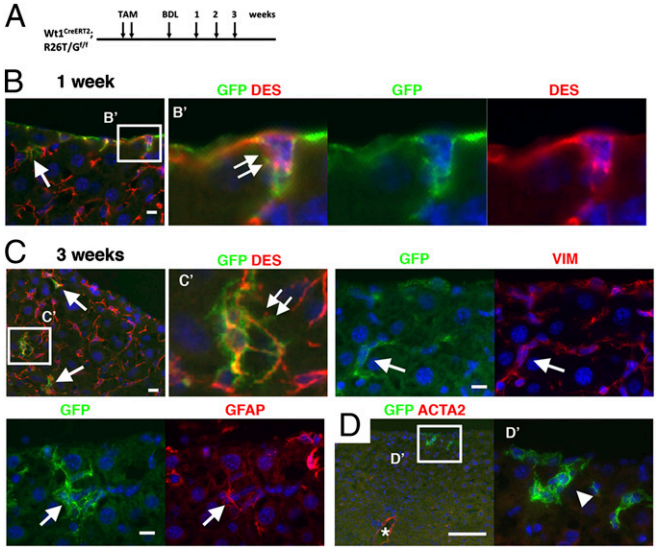

Fig. 5. Differentiation of MCs into HSCs in biliary fibrosis. (*A*) After labeling MCs in Wt1^{CreERT2};R26T/G^f mice by TAM injection, biliary fibrosis was induced by BDL. (*B–D*) Immunostaining. Double arrows indicate GFP$^+$ DES$^+$ MCs, which seem to begin migration inward from the liver surface 1 wk after BDL (*B*) and GFP$^+$ DES$^+$ HSCs having dendritic processes (*C*). Arrows indicates GFP$^+$ HSCs expressing DES, VIM, or GFAP. (*D*) An arrowhead and asterisk indicate ACTA2$^-$ GFP$^+$ HSCs and ACTA2$^+$ smooth muscle cells in the vein, respectively. Nuclei were counterstained with DAPI. [Scale bar, 10 μm (*B* and *C*) and 100 μm (*D*).]

and expression of these factors was only marginally induced by TGF-β in MCs, suggesting minor involvement of these transcription factors in liver MMT. Intriguingly, liver MCs did not express CDH1, a well-known target of EMT. However, peritoneal MCs were shown to decrease expression of CDH1 and cytokeratin while increasing SNAI1 and changing their shape to fibroblastic upon treatment with TGF-β (3). It remains to be determined whether MCs in the liver have different characteristics from those in other organs.

Faris et al. (29) isolated MCs from rat liver using OC2 and BD2 monoclonal antibodies and suggested that epithelial progenitor cell lines are derived from MCs. In the present study, mouse MCs isolated using the GPM6A antibody did not express hepatocyte markers throughout the culture period. In addition, our cell lineage analysis indicated that MCs do not differentiate into hepatocytes in vivo. Our data suggest the differentiation potential of MCs is limited to mesenchymal cells in injured liver.

In conclusion, during liver injury, liver MCs give rise to both HSCs and myofibroblasts by recapitulating their developmental lineage. Liver MMT may ultimately prove to be a novel therapeutic target for suppression of capsular liver fibrosis.

Materials and Methods

Mouse Models. $Wt1^{CreERT2}$, $Wt1^{GFPCre}$, $R26lacZ^{f}$, and $R26T/G^{f}$ were used (13, 24, 25). TAM (Sigma) dissolved in ethanol was emulsified in sesame oil at 12.5 μg/mL and was injected intraperitoneally to the mice (5–10 wk) at 100 μg/g body weight twice in a 3-d interval. One week after the last injection, mice were injected s.c. with 1 mL/kg body weight of CCl_4 mixed with mineral oil every 3 d 1–30 times (30). To suppress fibrosis, mice were treated with STR (TGF-βR2 Fc chimera) or mouse IgG2a isotype control (0.1 mg/kg body weight, $n = 3$) (R&D Systems) by i.p. injections 12 times every 3 d. To induce biliary fibrosis, the mice were subjected to BDL (28) and were similarly treated with STR or IgG2a five times every 3 d. Liver regeneration was induced by 70% PHx (10). The mice were used in accordance with protocols approved by the Institutional Animal Care and Use Committee of the University of Southern California.

Histological Analysis. Tissues were fixed with 4% (wt/vol) paraformaldehyde or 70% (vol/vol) ethanol and cryosections were prepared (8). The antibodies used in immunostaining are listed in Table S1. The primary antibodies were detected with secondary antibodies conjugated with fluorescent dyes. The sections were counterstained with DAPI. Tomato fluorescence was bleached with 3% H_2O_2 in methanol 30 min before immunostaining. Expression of LACZ was detected by either X-gal staining or immunohistochemistry (7). After X-gal staining, the sections were immunostained by using anti-DESMIN antibodies and SuperPicture Polymer detection kit (Invitrogen). The sections were visualized under the microscope and images were captured with digital cameras (Nikon).

Isolation and Culture of MCs. After partial digestion of whole liver lobes with 1 mg/mL pronase (Roche) in DMEM/F-12 medium for 20 min at 37 °C with gentle shaking, the cells were centrifuged at 1,700 × *g* for 5 min and were suspended in DMEM containing 10% FBS. After washing three times, the cells were incubated with anti-Gpm6a antibody at 1,500-fold dilution in DMEM for 15 min at 4 °C. After centrifugation, the cells were incubated with anti-rat IgG MicroBeads and were purified by autoMACS (Miltenyi Biotech) according to their instructions. MCs were plated on a collagen-coated dish in DMEM with low glucose containing 10% FBS, ITS (Gibco), and 50 ng/mL hydrocortisone. MCs were treated with 10 ng/mL TGF-β1 (T1654; Sigma), 20 ng/mL HGF (H1404), 10^{-6} M AngII (A9525), 1 μM RA (R2625), 0.01% ethanol, 50 ng/mL EGF (EA140; Chemicon), 100 ng/mL WNT3A (1324; R&D Systems), or 100 ng/mL DKK1 (5897) in the presence or absence of following chemical inhibitors: 5 μM SB431542 (04-0010; Stemgent), 10 μM SIS3 (566405; Calbiochem), 10 μM SB203580 (559389), 10 μM JNK inhibitor II (420128), 10 μM U0126 (9903; Cell Signaling), 100 nM Rapamycin (9904), or 0.1% DMSO.

Statistical Analysis. Statistical significance was estimated by Student *t* test. A level of $P < 0.05$ was considered statistically significant.

FACS, QPCR (Table S2), microarray analysis, immunostaining, X-gal staining, quantification, and isolation of HSCs are presented in *SI Materials and Methods*.

ACKNOWLEDGMENTS. We thank Dr. Hidekazu Tsukamoto for expert advice and guidance, Irving Garcia, Raul Lazaro, Kiki Ueno, and Bin Xie for technical assistance, and Bin Zhou and William Pu for providing Wt1 mice. This work was supported by National Institutes of Health Grant R01AA020753, pilot project funding from Grant P50AA011999, pilot project funding from Grant P30DK048522, and Grant R24AA12885.

1. Mutsaers SE (2004) The mesothelial cell. *Int J Biochem Cell Biol* 36(1):9–16.
2. Yung S, Li FK, Chan TM (2006) Peritoneal mesothelial cell culture and biology. *Perit Dial Int* 26(2):162–173.
3. Strippoli R, et al. (2008) Epithelial-to-mesenchymal transition of peritoneal mesothelial cells is regulated by an ERK/NF-kappaB/Snail1 pathway. *Dis Model Mech* 1(4-5):264–274.
4. Thiery JP, Acloque H, Huang RY, Nieto MA (2009) Epithelial-mesenchymal transitions in development and disease. *Cell* 139(5):871–890.
5. Patel P, et al. (2010) Smad3-dependent and -independent pathways are involved in peritoneal membrane injury. *Kidney Int* 77(4):319–328.
6. Chapman GB, Eagles DA (2007) Ultrastructural features of Glisson's capsule and the overlying mesothelium in rat, monkey and pike liver. *Tissue Cell* 39(5):343–351.
7. Asahina K, et al. (2009) Mesenchymal origin of hepatic stellate cells, submesothelial cells, and perivascular mesenchymal cells during mouse liver development. *Hepatology* 49(3):998–1011.
8. Asahina K, Zhou B, Pu WT, Tsukamoto H (2011) Septum transversum-derived mesothelium gives rise to hepatic stellate cells and perivascular mesenchymal cells in developing mouse liver. *Hepatology* 53(3):983–995.
9. Onitsuka I, Tanaka M, Miyajima A (2010) Characterization and functional analyses of hepatic mesothelial cells in mouse liver development. *Gastroenterology* 138(4):1525–1535, 1535, e1–e6.
10. Asahina K, et al. (2002) Pleiotrophin/heparin-binding growth-associated molecule as a mitogen of rat hepatocytes and its role in regeneration and development of liver. *Am J Pathol* 160(6):2191–2205.
11. Wilm B, Ipenberg A, Hastie ND, Burch JB, Bader DM (2005) The serosal mesothelium is a major source of smooth muscle cells of the gut vasculature. *Development* 132(23):5317–5328.
12. Que J, et al. (2008) Mesothelium contributes to vascular smooth muscle and mesenchyme during lung development. *Proc Natl Acad Sci USA* 105(43):16626–16630.
13. Zhou B, et al. (2008) Epicardial progenitors contribute to the cardiomyocyte lineage in the developing heart. *Nature* 454(7200):109–113.
14. Bataller R, Brenner DA (2005) Liver fibrosis. *J Clin Invest* 115(2):209–218.
15. Friedman SL (2008) Hepatic stellate cells: Protean, multifunctional, and enigmatic cells of the liver. *Physiol Rev* 88(1):125–172.
16. Knittel T, et al. (1999) Rat liver myofibroblasts and hepatic stellate cells: Different cell populations of the fibroblast lineage with fibrogenic potential. *Gastroenterology* 117(5):1205–1221.
17. Dranoff JA, Wells RG (2010) Portal fibroblasts: Underappreciated mediators of biliary fibrosis. *Hepatology* 51(4):1438–1444.
18. Bhunchet E, Wake K (1992) Role of mesenchymal cell populations in porcine serum-induced rat liver fibrosis. *Hepatology* 16(6):1452–1473.
19. Barclay AN, Wright GJ, Brooke G, Brown MH (2002) CD200 and membrane protein interactions in the control of myeloid cells. *Trends Immunol* 23(6):285–290.
20. Wu DF, et al. (2007) Membrane glycoprotein M6a interacts with the micro-opioid receptor and facilitates receptor endocytosis and recycling. *J Biol Chem* 282(30):22239–22247.
21. Bochmann L, et al. (2010) Revealing new mouse epicardial cell markers through transcriptomics. *PLoS ONE* 5(6):e11429.
22. von Gise A, et al. (2011) WT1 regulates epicardial epithelial to mesenchymal transition through β-catenin and retinoic acid signaling pathways. *Dev Biol* 356(2):421–431.
23. Xu J, Lamouille S, Derynck R (2009) TGF-β-induced epithelial to mesenchymal transition. *Cell Res* 19(2):156–172.
24. Muzumdar MD, Tasic B, Miyamichi K, Li L, Luo L (2007) A global double-fluorescent Cre reporter mouse. *Genesis* 45(9):593–605.
25. Soriano P (1999) Generalized lacZ expression with the ROSA26 Cre reporter strain. *Nat Genet* 21(1):70–71.
26. Yata Y, Gotwals P, Koteliansky V, Rockey DC (2002) Dose-dependent inhibition of hepatic fibrosis in mice by a TGF-β soluble receptor: Implications for antifibrotic therapy. *Hepatology* 35(5):1022–1030.
27. Popov Y, Schuppan D (2009) Targeting liver fibrosis: Strategies for development and validation of antifibrotic therapies. *Hepatology* 50(4):1294–1306.
28. Yang MD, et al. (2012) Rosmarinic acid and baicalin epigenetically de-repress Pparγ in hepatic stellate cells for their anti-fibrotic effect. *Hepatology* 55(4):1271–1281.
29. Faris RA, et al. (1994) Isolation, propagation, and characterization of rat liver serosal mesothelial cells. *Am J Pathol* 145(6):1432–1443.
30. Higashiyama R, et al. (2009) Negligible contribution of bone marrow-derived cells to collagen production during hepatic fibrogenesis in mice. *Gastroenterology* 137(4):1459–1466, e1.